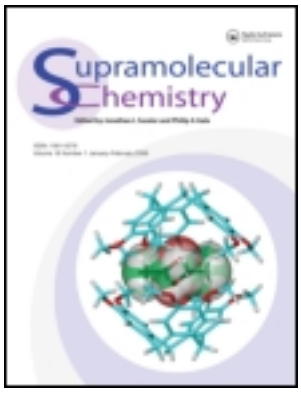

Supramolecular Chemistry
Publication details, including instructions for authors and subscription information:
http://www.tandfonline.com/loi/gsch20

Solid-state structures of ureidoimidazoles

Andrea M. McGhee [a], Jeffrey P. Plante [a], Colin A. Kilner [a] & Andrew J. Wilson [a b]
[a] School of Chemistry, University of Leeds, Leeds, UK
[b] Astbury Centre for Structural Molecular Biology, University of Leeds, Leeds, UK

Available online: 15 Apr 2011

To cite this article: Andrea M. McGhee, Jeffrey P. Plante, Colin A. Kilner & Andrew J. Wilson (2011): Solid-state structures of ureidoimidazoles, Supramolecular Chemistry, 23:6, 470-479

To link to this article: http://dx.doi.org/10.1080/10610278.2010.550289

Supramolecular Chemistry
Vol. 23, No. 6, June 2011, 470–479

Taylor & Francis
Taylor & Francis Group

Solid-state structures of ureidoimidazoles

Andrea M. McGhee[a], Jeffrey P. Plante[a], Colin A. Kilner[a] and Andrew J. Wilson[ab]*

[a]*School of Chemistry, University of Leeds, Leeds, UK;* [b]*Astbury Centre for Structural Molecular Biology, University of Leeds, Leeds, UK*

(*Received 25 October 2010; final version received 20 December 2010*)

This work outlines the synthesis and solid-state structures of a series of ureidoimidazole derivatives. The ureidoimidazoles all adopt a common tautomeric configuration and possess remarkably consistent features of supramolecular organisation that are affected by both steric factors and proximal hydrogen-bonding functionality.

Keywords: hydrogen-bonding; linear arrays; self assembly

Introduction

The design and synthesis of hydrogen-bonding motifs exhibiting well-defined supramolecular organisation both in solution and in solid state is an ongoing area of interest (*1–8*). Hydrogen-bonding motifs are important building blocks for the assembly of supramolecular polymers (*8–10*) and more generally of self-assembling gelators (*11*, *12*) which attract attention as tuneable 'smart materials'. They also play a central role in crystalline assemblies, which are significant in a number of areas including polymorphism of active pharmaceutical ingredients (*13*) and solid-state reactivity (*14*). Furthermore, solid-state structures can provide valuable information on molecular recognition behaviour in solution. Our group have initiated an investigation concerned with the development of linear arrays of hydrogen bonds (*15*, *16*) to be used as components of supramolecular polymers (*8–10*). The current work focuses on the ureidoimidazole donor–donor–acceptor motif previously shown by us to exhibit conformer independent heterodimerisation with the complementary amidoisocytosine acceptor–acceptor–donor array (*16*). Although our prior studies have illustrated negligible self-association of the ureidoimidazole motif in solution, the current results reveal an unusual mode of self-assembly in the solid state for a series of compounds; this is remarkably conserved across the series and subtly modulated through both steric effects and proximal hydrogen-bonding groups.

Results and discussion

The ureidoimidazole derivatives **1**, **2** and **3a–c** were synthesised using standard procedures as illustrated in Scheme 1.

Single crystals of each compound suitable for a diffraction study were obtained as described in the Experimental section, and were subjected to crystallographic structure determination. The crystal structure of compound **1** has been previously disclosed by us (*16*). Compound **1** crystallises in the monoclinic $P2_1/n$ space group, with one molecule present in the asymmetric unit. Of the two conformational possibilities, intramolecular urea NH to imidazole N hydrogen bonded and intramolecular urea carbonyl to imidazole NH hydrogen bonded, only the latter is observed (Figure 1(a)). The packing of compound **1** is mediated by intermolecular hydrogen bonds, which, based on the intermolecular heteroatom hydrogen distances, would be described as weak hydrogen bonds. Bifurcated hydrogen bonding between urea NHs and the imidazole nitrogen is observed with each monomer perpendicular to two others, while the backface of the molecule interacts through carbonyl to imidazole NH hydrogen bonding creating an infinite 2D structure (Figure 1(b)). Van der Waals packing is observed between sheets (Figure 1(c)). Similarly, according to our original report (*16*), Barboiu reported a structure of compound **1** that is virtually identical to the one we reported (*17*).

Compound **2** crystallises in the monoclinic *C2/c* space group, with one molecule present in the asymmetric unit. Again, only intramolecular urea carbonyl to imidazole NH hydrogen bonding is observed (Figure 2(a)). As for compound **1**, weak bifurcated hydrogen bonding between urea NHs and the imidazole nitrogen is observed with each monomer perpendicular to two others; however, no hydrogen bonds are observed involving the carbonyl and imidazole NHs on the opposite side of the molecule to the DDA array (Figure 2(b) and (c)). Therefore, infinite 1D chains are observed, which are packed in the second and third dimensions through aromatic $\pi-\pi$ edge to face (ArC–H–π interaction), $\pi-\pi$ face to face and Van der Waals interactions (Figure 2(c)–(e)).

Compound **3a** crystallises in the monoclinic $P2_1/n$ space group, with two molecules and two solvent methanol

*Corresponding author. Email: a.j.wilson@leeds.ac.uk

ISSN 1061-0278 print/ISSN 1029-0478 online

DOI: 10.1080/10610278.2010.550289
http://www.informaworld.com

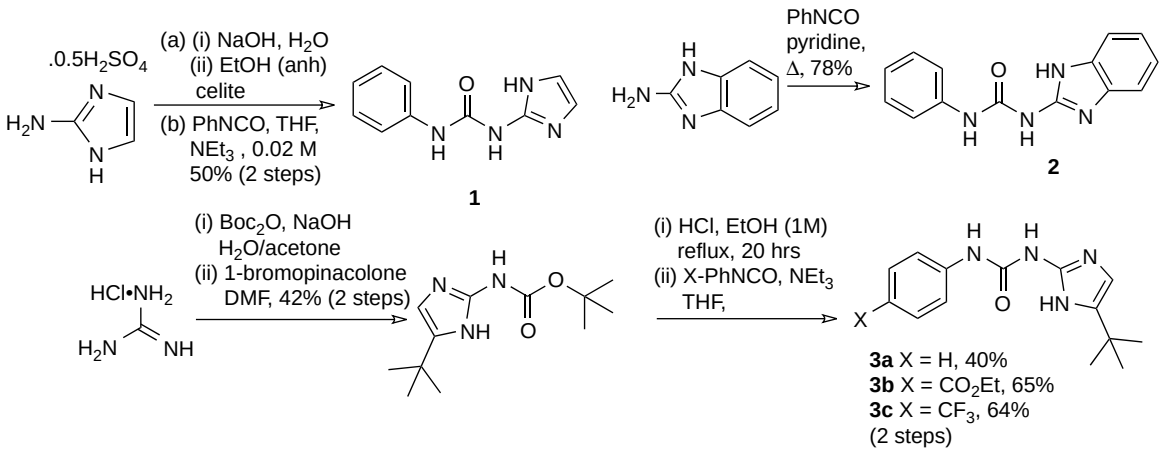

Scheme 1. Synthesis of compounds **1**, **2** and **3a**–**c**.

molecules present in the asymmetric unit. The conformations of each molecule of **3a** are only subtly different. As for the first two examples, only intramolecular urea carbonyl to imidazole NH hydrogen bonding is observed; however, the packing structure is significantly different in the presence of solvent (Figure 3(a)). The same core mode of dimerisation that is observed for **1** and **2** is observed for **3a** in that urea NH bifurcated hydrogen bonding with the imidazole is observed; however, in this instance, the solvent molecule acts as a bridge – the interactions are therefore significantly stronger as evidenced by the shorter intermolecular distances – and a coplanar rather than the perpendicular arrangement of **3a** is observed, i.e. a self-complementary dimer is observed bridged by two methanol molecules (Figure 3(b) and (c)). The infinite 1D polymer is propagated through self-complementary hydrogen bonds involving the carbonyl and imidazole NHs on the opposite side of the molecule to the DDA array as is the case for compound **1**. Packing in the second and third dimensions is mediated by Van der Waals interactions (Figure 3(d)).

Compound **3b** crystallises in the triclinic $P\bar{1}$ space group, with two molecules and three solvent methanol molecules present in the unit cell. One of the methanol molecules is disordered over two equally occupied positions. There are only minor differences between the structures of the individual monomer units. Again, the conformation of **3b** is determined by intramolecular urea carbonyl to imidazole NH hydrogen bonding, and the DDA array present in the structure is the same as the other compounds (Figure 4(a)). The solid-state assembly is similar in nature to **3a**. The principle difference is that the infinite 1D polymer is propagated through self-complementary hydrogen bonds involving the carbonyl of the ester (as opposed to the urea) and imidazole NH – an additional hydrogen bond from the urea carbonyl to a solvent CH is also observed (Figure 4(b) and (c)). Packing in the second and third dimensions is mediated by Van der Waals interactions (Figure 4(d)).

Compound **3c** crystallises in the triclinic $P\bar{1}$ space group, with two molecules and two solvent methanol molecules present in the asymmetric unit. Each molecule of **3c** is only subtly different. Like all other examples, a single defined conformation is observed, which is dictated by the intramolecular hydrogen bonding (Figure 5(a)). The packing structure of **3c** is very similar to compound **3a**, and all the same hydrogen-bonding features are present within the observed infinite 1D polymer with Van der Waals interactions mediating the packing in the second and third dimensions (Figure 5(b)–(d)).

Overall, the salient solid-state assembly properties of the ureidoimidazole series are summarised in Figure 6. Each structure adopts a common conformation mediated by intramolecular hydrogen bonding between the imidazole NH and the carbonyl functionality of the urea motif to present a donor–donor–acceptor array. In the absence of solvent, direct interaction of each urea group with the acceptor on the imidazole of an adjacent molecule is observed. The perpendicular orientation (which presumably results from steric constraints imposed by R^1) results in an infinite 1D chain as is observed for **1** and **2** (Figure 6(a)). Assembly for this series can be propagated in a second dimension through self-complementary hydrogen bonding between the rear faces as for **1**. This feature is 'switched-off' with sterically bulky ureidoimidazoles as for **2** – the R^2 group in Figure 6(a) is clearly positioned to influence packing of adjacent molecules. In the presence of methanol, stronger hydrogen bonding is observed and the solvent acts as a bridge between the urea NHs and imidazole Ns on two coplanar ureidoimidazole motifs as is observed for **3a**–**c** (Figure 6(b)). The infinite 1D chain is propagated through self-complementary hydrogen bonding between the rear faces. This interaction is the same as that which is observed to mediate propagation in the second dimension, when solvent is absent (i.e. compound **1**), although it should be noted that the presence of additional hydrogen-bonding functionality on the ureidoimidazole

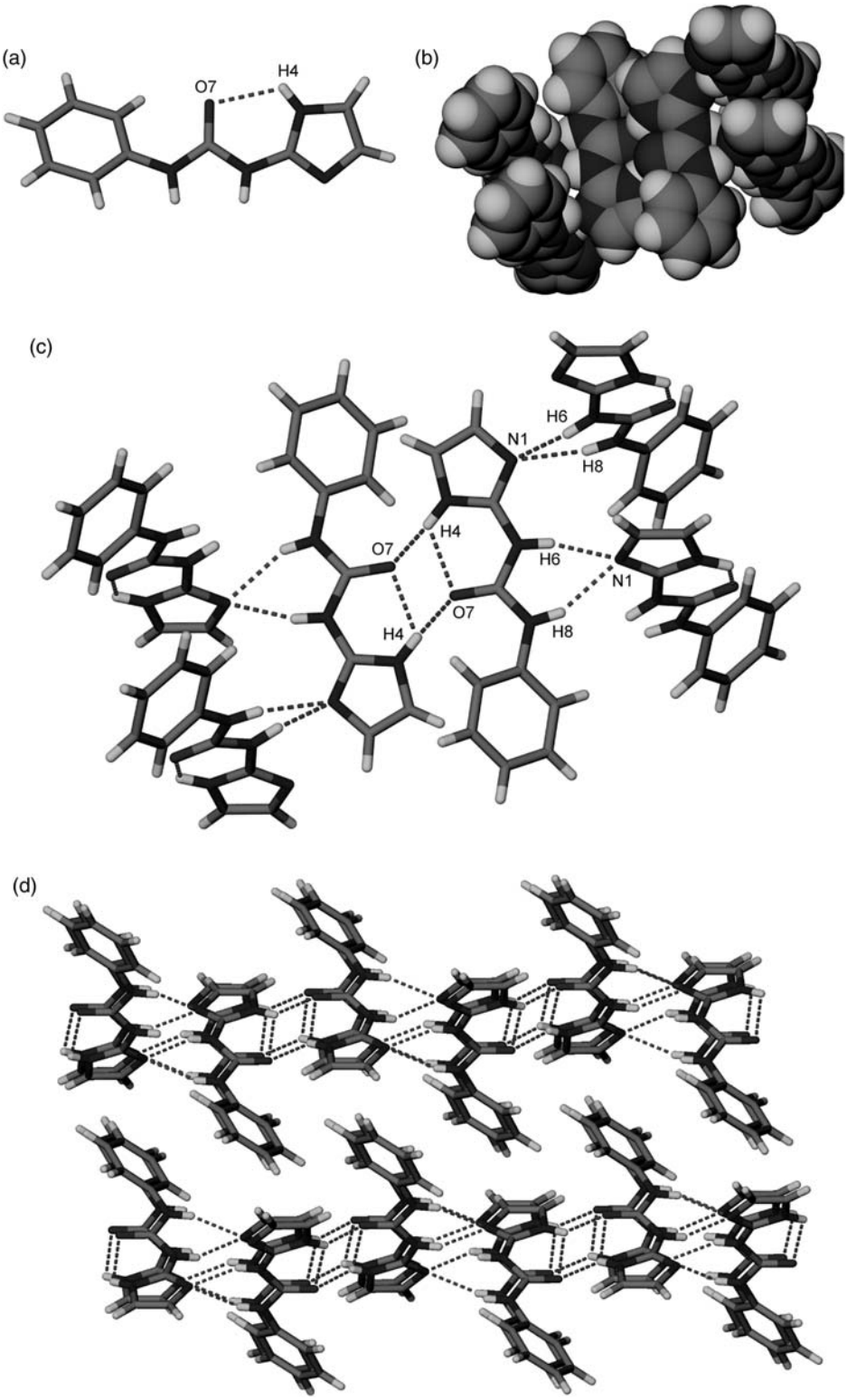

Figure 1. (a) X-ray crystal structure of compound **1**, (b) structure packing diagram of compound **1** shown in CPK format, (c) stick representation of (b), key distances: H4–O7 2.31 Å (intramolecular), H4–O7 2.11 Å, N1–H6 2.09 Å, N1–H8 2.25 Å (intermolecular), (d) solid-state structure of **1** illustrating intrasheet packing.

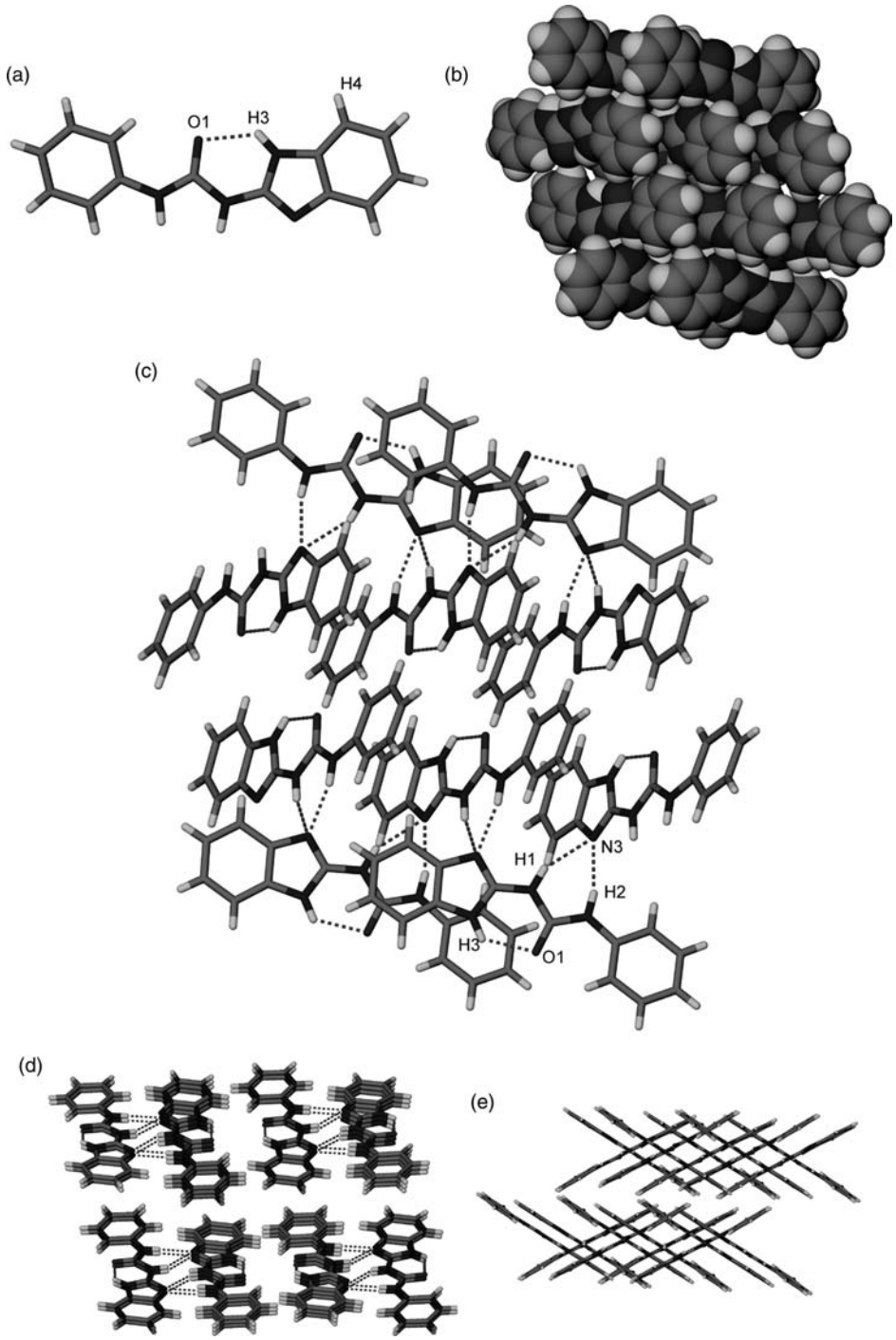

Figure 2. (a) X-ray crystal structure of compound **2**, (b) structure packing diagram of compound **2** shown in CPK format, (c) stick representation of (b), key distances: H3–O1 2.04 Å (intramolecular), H2–N3 2.19 Å, H1–N3 2.11 Å (intermolecular), (d) and (e) solid-state structure of **2** illustrating intrasheet packing.

can play a role as is the case for **3b**, where $Y = CO_2Et$ (the size of R^2 is also anticipated to influence assembly).

Conclusions

We have reported the synthesis and solid-state structure of a series of ureidoimidazole motifs. In solution (chloroform), the ureidoimidazole motif has been shown by us to participate in self-association to a negligible extent ($<10\,M^{-1}$) (*16*); however, hydrogen bonding plays a significant role in determining the solid-state structures that are observed. In the absence of a bridging solvent, the intermolecular distances for these interactions indicate that

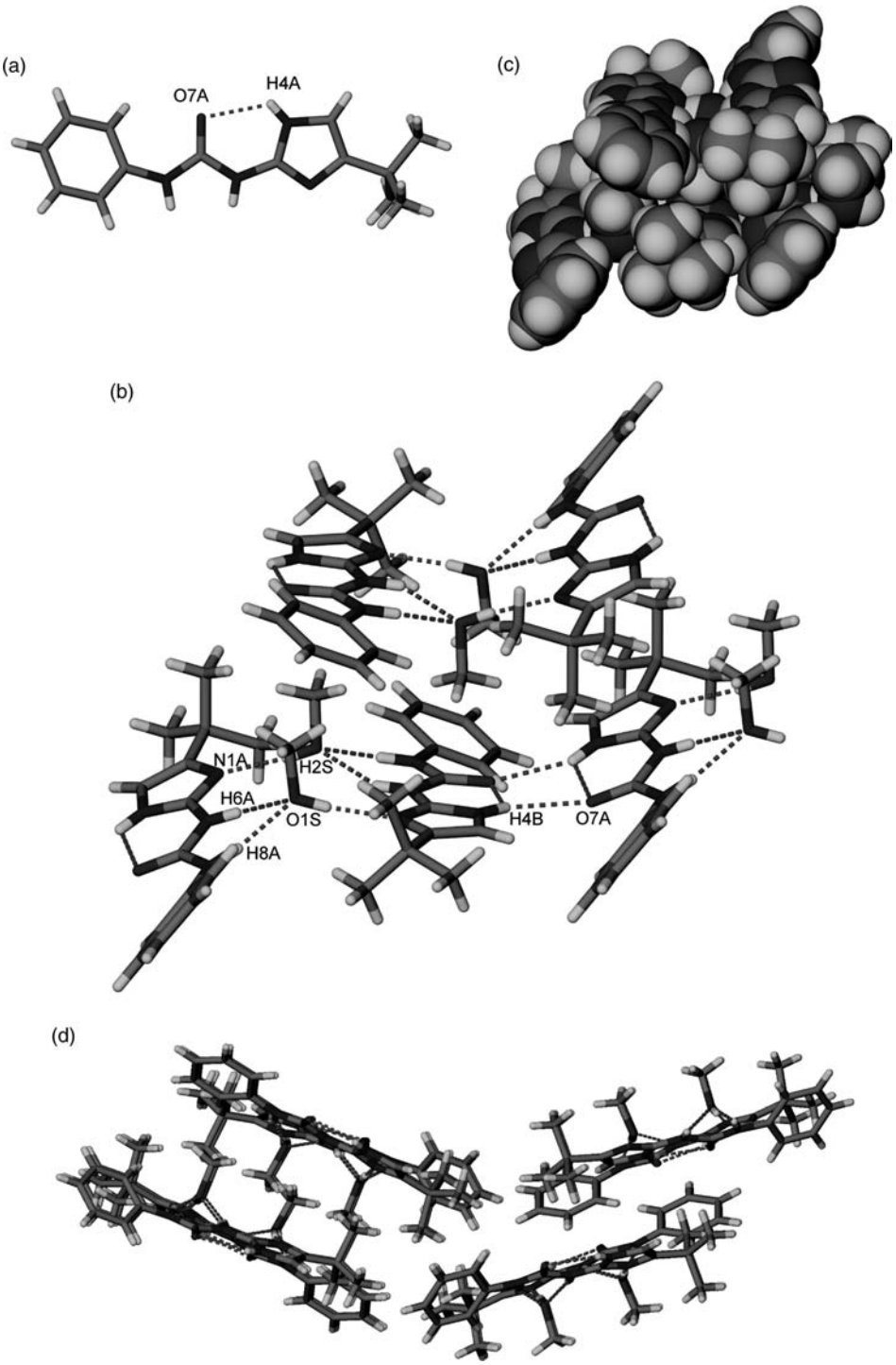

Figure 3. (a) X-ray crystal structure of compound **3a**, (b) structure packing diagram of compound **3a** shown in CPK format, (c) stick representation of (b), key distances: O7A–H4A 2.29 Å (intramolecular), N1A–H2S 1.89 Å, H6A–O1S 2.16 Å, H8A–O1S 2.03 Å, O7A–H4B 2.29 Å (intermolecular), (d) solid-state structure of **3a** illustrating intrasheet packing.

these interactions are weak, which reinforces the solution observations. The urea motif has a strong tendency to engage in bifurcated hydrogen bonding involving both its NHs (*2*), and this seems to play a prominent role here in controlling the solid-state assembly. These observations will be used in our ongoing efforts to design and synthesise novel linear arrays of hydrogen-bonding groups for supramolecular assembly.

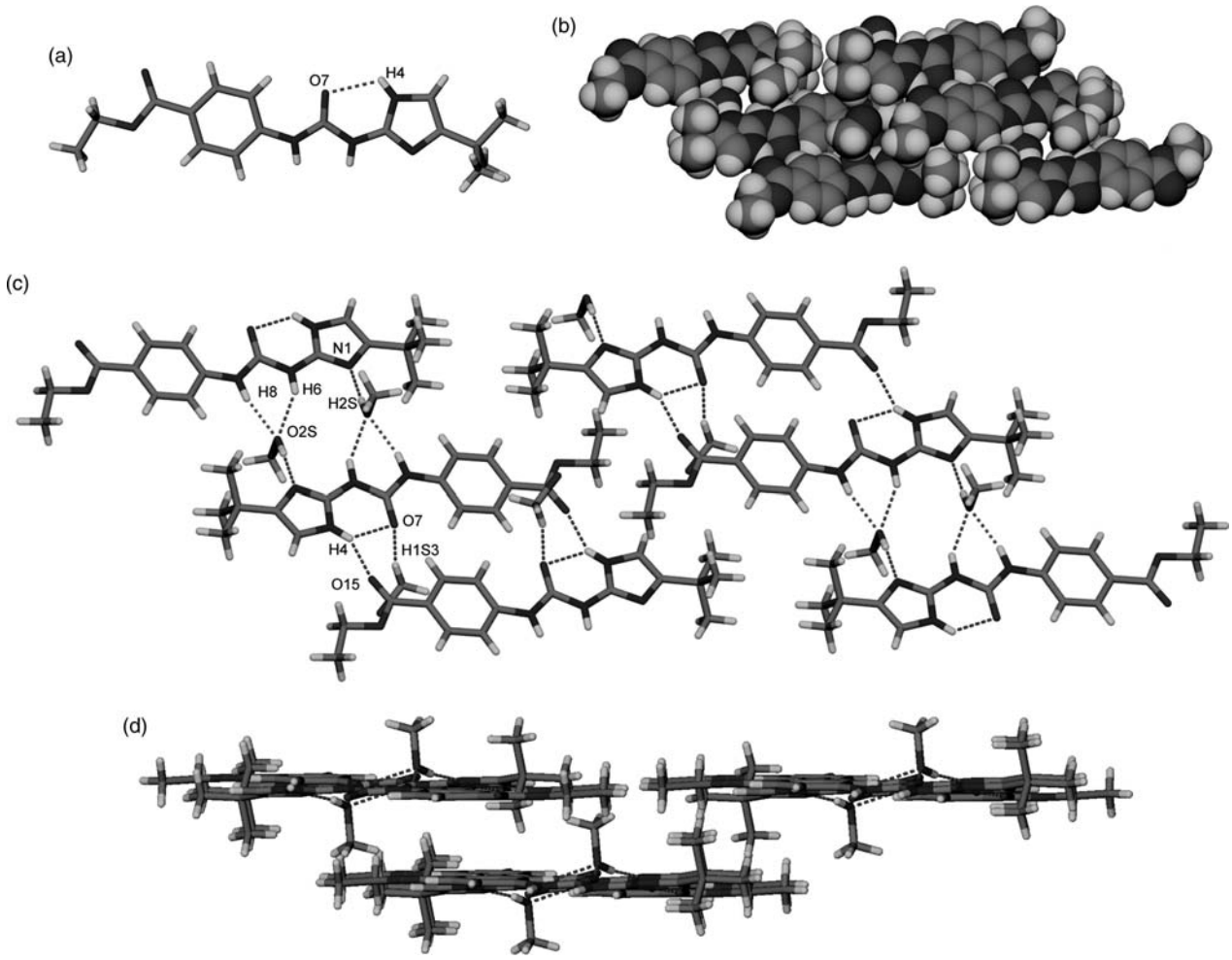

Figure 4. (a) X-ray crystal structure of compound **3b**, (b) structure packing diagram of compound **3b** shown in CPK format, (c) stick representation of (b), key distances: H4–O7 2.26 Å (intramolecular), N1–H1S 1.87 Å, H6–O1S 2.14 Å, H8–O2S 2.01 Å, H4–015 2.13 Å, H1S3–07 2.05 Å (intermolecular), (d) solid-state structure of **3b** illustrating intrasheet packing.

Experimental

All reagents were purchased from Aldrich or Alfa Aesar and used without further purification unless otherwise stated. Where anhydrous solvents were required, THF was freshly distilled from sodium benzophenone ketyl radical, CH_2Cl_2 was freshly distilled from calcium hydride and $CHCl_3$ was freshly distilled from calcium chloride under a nitrogen atmosphere. Anhydrous DMF was obtained 'sure-sealed' from Sigma-Aldrich (Poole, Dorset, UK). Triethylamine was distilled from calcium hydride and stored, under nitrogen, over potassium hydroxide pellets. All non-aqueous reactions were carried out under a nitrogen atmosphere. Analytical thin layer chromatography was conducted using Merck Kieselgel 0.25 mm silica gel precoated aluminium plates with fluorescent indicator active at UV_{245}. Purification by column chromatography was carried out using Merck Kieselgel 60 silica gel. NMR spectra were obtained using Bruker DMX500 or Bruker AMD300 spectrometers operating at 500 or 300 MHz for ^1H spectra and 125 or 75 MHz for ^{13}C spectra as stated. Proton spectra are referenced to TMS at 0.00 ppm, and carbon spectra to $CDCl_3$ at 77.4 ppm, unless otherwise stated. Melting points were determined using a Griffin D5 variable temperature apparatus and are uncorrected. IR spectra were obtained using Perkin-Elmer FTIR spectrometer. Microanalysis was carried out on a Carlo Erba Elemental Analyser MOD 1106 instrument. High Resolution Mass Spectra (HRMS) were recorded on a Micromass GCT Premier using electron impact ionisation or a Bruker Daltonics micrOTOF using electro spray ionisation (ESI).

N-tert-Butoxycarbonylguanidine (*16*)

The title compound was prepared as described previously (*16*).

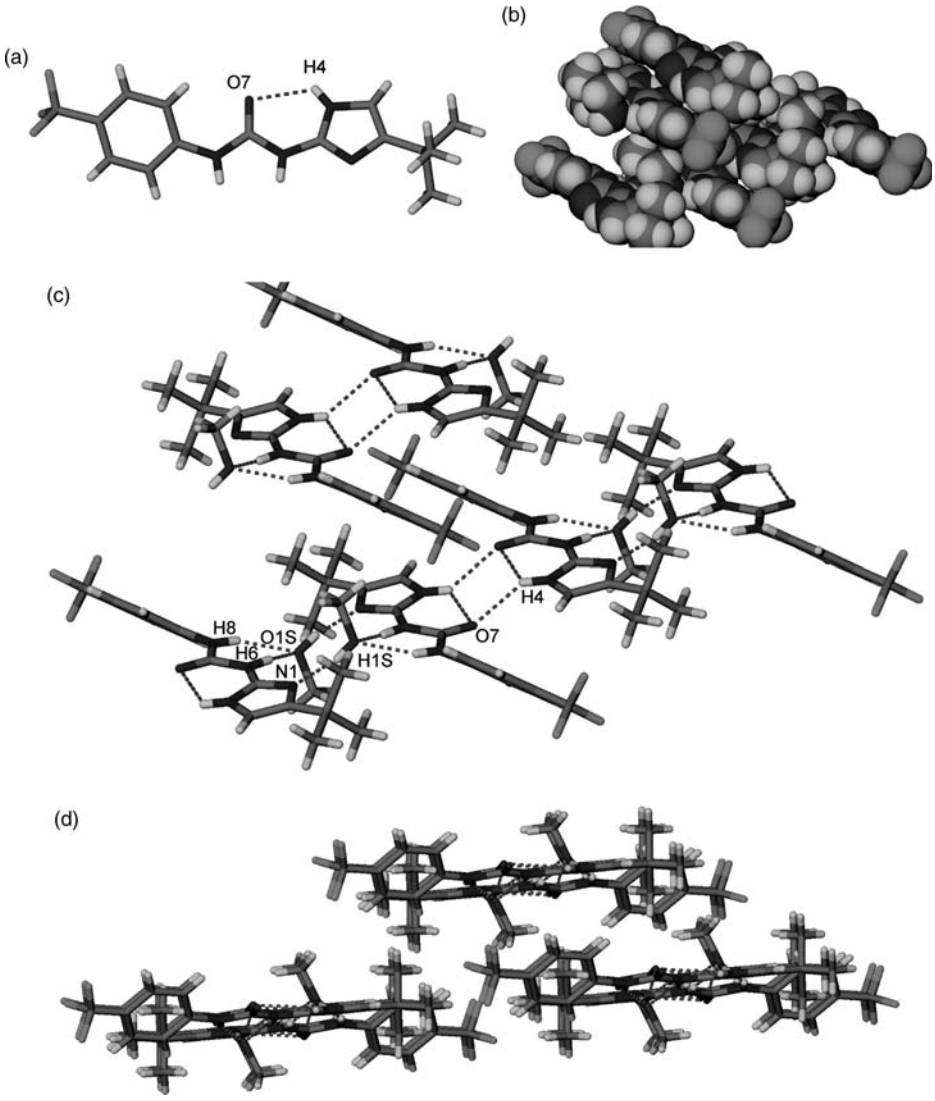

Figure 5. (a) X-ray crystal structure of compound **3c**, (b) structure packing diagram of compound **3c** shown in CPK format, (c) stick representation of (b), key distances: H4–O7 2.35 Å (intramolecular), N1–H1S 1.88 Å, H6–O1S 1.99 Å, H8–O1S 2.12 Å, H4–O7 2.26 Å (intermolecular), (d) solid-state structure of **3c** illustrating intrasheet packing.

2-*tert*-Butoxyamido-4-*tert*-butylimidazole (*16*)

The title compound was prepared as described previously (*16*).

***N*-Phenyl-*N*′-(imidazo-2-yl)urea 1**

The title compound was prepared as described previously (*16*).

1-(1*H*-Benzo[d]imidazol-2-yl)-3-phenylurea 2

A stirred solution of 2-aminobenzimidazole (0.500 g, 3.75 mmol) in anhydrous pyridine under nitrogen was brought to 100°C. Phenylisocyanate (0.387 ml, 0.4245 g, 3.57 mmol) was then added, and stirring was continued. After 20 min, a precipitate began to form, and after 1 h the reaction mixture was cooled and filtered to give a white solid (0.340 g). The filtrate was then poured into water to give a precipitate (0.366 g) that was filtered and dried. Both samples were found to be identical giving a total yield of product (0.706 g, 87%) as a white solid, which was not purified further, m.p. decomposes > 236.0°C; δ_H (500 MHz, DMSO-d_6); 7.01 (1H, t, $J = 7.0$, ArCH), 7.06 (2H, dd, $J = 5.5$, 3.2, ArCH), 7.31 (2H, t, $J = 8.0$, ArCH), 7.37 (2H, dd, $J = 5.5$, 3.2, ArCH), 7.57 (2H, d, $J = 7.7$, ArCH), 9.57 (1H, br s, NH) 11.32 (1H, br s, NH); δ_C (75 MHz, DMSO-d_6) 118.4, 118.5, 118.9, 121.3, 122.1, 122.7, 129.1, 139.69, 140.0, 150.0, 152.9; ν_{max}/cm^{-1}; 3278

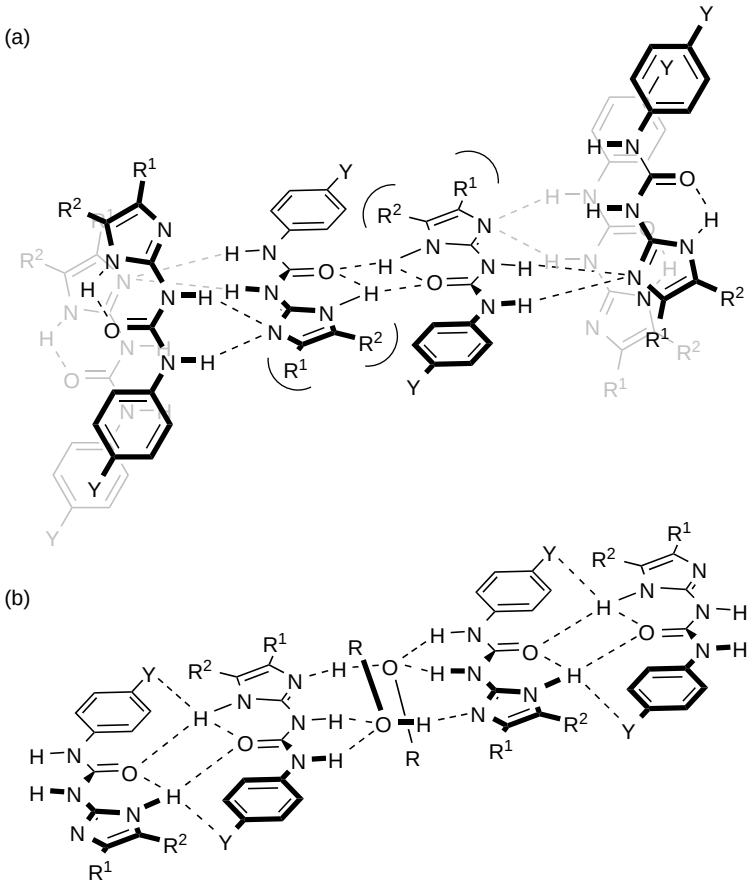

Figure 6. Solid-state assembly behaviour of ureidoimidazole compounds (a) **1** and **2**, (b) **3a**–**c**.

(NH), 1717 (CO), 1599 (CO), 1557, 1498, 1447, 1313, 1233; *m/z* (ESI-MS) 253 $[M + H]^+$.

*General procedure: synthesis of ureido-4-*tert*-butylimidazoles*

2-*tert*-Butoxyamido-**4**-*tert*-butylimidazole (1.0 equiv.) was stirred in 20% HCl/EtOH (100 ml per 1.0 g of starting material) for 1 h. The solution was concentrated, and the residue was dried under vacuum for 1 h. The resulting material was dissolved in dry THF (40 ml per 1.0 g of material) at room temperature under N_2, and triethylamine (1.5 equiv.) was added. The reaction mixture was heated to reflux, and the appropriate *iso*cyanate (1.0 equiv., 1.0 M in THF) was added dropwise. The reaction mixture was stirred at reflux for 16 h. After cooling to room temperature, the volatiles were removed under reduced pressure, and the residue was partitioned between EtOAc and water. The layers were separated, and the aqueous phase was extracted with EtOAc. The combined organics were washed with aqueous saturated NH_4Cl, aqueous saturated $NaHCO_3$ and brine, dried (Na_2SO_4) and concentrated under reduced pressure before purification by column chromatography.

1-(4-*tert*-Butyl-1*H*-imidazol-2-yl)-3-phenylurea 3a (*16*)

Adopting minor modifications to our published method (*16*), the general procedure using 2-*tert*-butoxyamido-4-*tert*-butylimidazole (1.94 g, 10.0 mmol) and phenyl*iso*cyanate (1.08 ml, 10.0 mmol) provided a yellow/brown solid, which was purified by column chromatography (gradient elution: 2:3 EtOAc–hexane to 1:19 MeOH–EtOAc) and crystallised (1:1 MeOH:MeCN–H_2O) to give the title compound (1.04 g, 40%) as a cream coloured solid; m.p. 70–73°C (MeOH:MeCN–H_2O), [Lit. decomp > 147° C]; R_f 0.24 (1:19 MeOH–CH_2Cl_2); δ_H (500 MHz, $CDCl_3$); 7.34 (2H, d, $J = 7.7$ Hz, ArCH), 7.26 (2H, d, $J = 7.7$ Hz, ArCH), 7.04 (1H, t, $J = 7.7$ Hz, ArCH), 6.29 (1H, s, ArCH), 1.25 (9H, s, ^{t}Bu); δ_C (75 MHz, $CDCl_3$); 154.9, 144.3, 138.6, 128.9, 123.3, 120.1, 119.8, 30.6, 29.7; ν_{max}/cm^{-1} 3281, 2960, 1669, 1592, 1551, 1499, 1449, 1310, 1238, 1198, 1156, 1082; ESI-HRMS found *m/z* 259.1553 $[M + H]^+$, $C_{14}H_{19}N_4O$ requires 259.1553.

Ethyl 4-(3-(4-*tert*-butyl-1*H*-imidazol-2-yl)ureido)benzoate 3b

The general procedure, using 2-*tert*-butoxyamido-4-*tert*-butylimidazole (820 mg, 3.4 mmol) and 4-ethoxycarbonylphenyl*iso*cyanate (721 mg, 3.8 mmol) provided a pale yellow solid that was purified by column chromatography (1:1 EtOAc–hexane) to give the title compound (804 mg, 65%) as a cream coloured solid; R_f 0.17 (EtOAc); δ_H (500 MHz, $CDCl_3$); 7.95 (2H, d, $J = 8.7$ Hz, ArCH), 7.47 (2H, d, $J = 8.7$ Hz, ArCH), 6.31 (1H, s, CHN), 4.35 (2H, q, $J = 7.2$ Hz, CH_3CH_2), 1.38 (3H, t, $J = 7.2$ Hz, CH_3CH_2), 1.29 (9H, s, ^{t}Bu); δ_C (75 MHz, DMSO-d_6); 165.8, 154.8, 144.9, 140.0, 130.7, 122.9, 117.7, 107.4, 60.6, 31.0, 29.9, 14.6; ν_{max}/cm^{-1} 3312, 2963, 1696, 1591, 1541, 1273, 1172, 1105 cm^{-1}; ESI-HRMS found *m/z* 331.1760 $[M + H]^+$, $C_{17}H_{23}N_4O_3$ requires 331.1765.

1-(4-*tert*-Butyl-1*H*-imidazol-2-yl)-3-(4-(trifluoromethyl)phenyl)urea 3c

The general procedure using 2-*tert*-butoxyamido-4-*tert*-butylimidazole (842 mg, 3.50 mmol) and 4-trifluoromethylphenyl*iso*cyanate (0.53 ml, 3.8 mmol) provided a pale yellow solid that was purified by column chromatography (2:3 EtOAc–hexane to EtOAc) and crystallised (1:1 MeOH–MeCN) to give the title compound (729 mg, 64%) as a colourless solid; m.p. 178–181°C (1:1 MeOH–MeCN); R_f 0.65 (EtOAc); δ_H (300 MHz, $CDCl_3$); 7.48 (2H, d, $J = 8.7$ Hz, ArCH), 7.42 (2H, d, $J = 8.7$ Hz, ArCH), 6.24 (1H, s, CHN), 1.23 (9H, s, ^{t}Bu); δ_C (75 MHz, $CDCl_3$); 155.3, 145.2, 143.6, 141.8, 126.3, 124.6 (q), 122.4, 118.5, 108.3, 30.5, 29.6; ν_{max}/cm^{-1} 3391, 2958, 1712, 1598, 1541, 1445, 1412, 1320, 1183, 1155, 1110, 1071, 1060, 1016, 987, 885; ESI-HRMS found *m/z* 327.1420 $[M + H]^+$, $C_{15}H_{18}F_3N_4O$ requires 327.1427.

Crystal structure determination for 1

The single crystal diffraction study for compound **1** has been reported previously (*16*). We note that, since the publication of our paper, a further report of the structure of **1** has appeared in the literature (*17*).

Crystal structure determination for 2

Single crystals were grown by the slow evaporation of a solution of **2** in chloroform/methanol. X-ray diffraction data were collected at the University of Leeds using a Bruker APEX2 instrument. Crystal data: $C_{14}H_{12}N_4O$, $M = 252.27$, crystal size $0.40 \times 0.40 \times 0.10$ mm, Monoclinic, $a = 24.2248(6)$, $b = 6.9079(2)$, $c = 16.2372(5)$ Å, $\beta = 119.482(2)°$, $U = 2365.33(12)$ Å^3, $T = 150(2)$ K, $C2/c$, $Z = 6$, $\mu = 0.108$ mm^{-1}, $\lambda = 0.71073$ Å [Mo Kα], 21,752 reflections measured, 3739 unique ($R_{int} = 0.0287$), observed 2957 ($I > 2\sigma(I)$). The final R_1 was 0.0418 (observed reflections 0.0580) and $wR(F^2)$ was 0.1144 (all data 0.1333) for 175 parameters. CCDC 795260 contains the supplementary crystallographic data for this paper. These data can be obtained free of charge from the Cambridge Crystallographic Data Centre via www.ccdc.cam.ac.uk/data_request/cif.

Crystal structure determination for 3a

Single crystals were grown by the slow evaporation of a solution of **3a** in moist acetonitrile/methanol. X-ray diffraction data were collected at the University of Leeds using a Bruker APEX2 instrument. Crystal data: $C_{15}H_{22}N_4O_2$, $M = 290.37$, crystal size $0.33 \times 0.15 \times 0.05$ mm, Monoclinic, $a = 12.0588(9)$, $b = 9.5465(7)$, $c = 29.231(2)$ Å, $\beta = 96.888(4)°$, $U = 3340.8(4)$ Å^3, $T = 150(2)$ K, $P2_1/n$, $Z = 8$, $\mu = 0.079$ mm^{-1}, $\lambda = 0.71073$ Å [Mo Kα], 58508 reflections measured, 8178 unique ($R_{int} = 0.042$), observed 5905 ($I > 2\sigma(I)$). The final R_1 was 0.0562 (observed reflections 0.0839) and $wR(F^2)$ was 0.1398 (all data 0.1523) for 413 parameters. CCDC 795261 contains the supplementary crystallographic data for this paper. These data can be obtained free of charge from the Cambridge Crystallographic Data Centre via www.ccdc.cam.ac.uk/data_request/cif.

Crystal structure determination for 3b

Single crystals were grown by the slow evaporation of a solution of **3b** in moist acetonitrile/methanol. X-ray diffraction data were collected at the University of Leeds using a Bruker APEX2 instrument. Crystal data: $C_{37}H_{56}N_8O_9$, $M = 756.9$, crystal size $0.35 \times 0.22 \times 0.04$ mm, Triclinic, $a = 8.0694(11)$, $b = 9.3523(13)$, $c = 14.6137(18)$ Å, $\alpha = 99.815(5)°$, $\beta = 103.015(5)°$, $\gamma = 102.771(5)°$, $U = 1019.4(2)$ Å^3, $T = 150(2)$ K, $P\bar{1}$, $Z = 1$, $\mu = 0.089$ mm^{-1}, $\lambda = 0.71073$ Å [Mo Kα], 19,367 reflections measured, 5107 unique ($R_{int} = 0.0272$), observed 3904 ($I > 2\sigma(I)$). The final R_1 was 0.0587 (observed reflections 0.0587) and $wR(F^2)$ was 0.1664 (all data 0.1798) for 247 parameters. CCDC 795262 contains the supplementary crystallographic data for this paper. These data can be obtained free of charge from the Cambridge Crystallographic Data Centre via www.ccdc.cam.ac.uk/data_request/cif.

Crystal structure determination for 3c

Single crystals were grown by the slow evaporation of a solution of **3c** in moist acetonitrile/methanol. X-ray diffraction data were collected at the University of Leeds using a Bruker APEX2 instrument. Crystal data: $C_{16}H_{21}F_3N_4O_2$, $M = 358.37$, crystal size $0.27 \times 0.21 \times 0.06$ mm, Triclinic, $a = 7.5470(9)$, $b = 11.2615(13)$, $c = 11.8882(12)$ Å, $\alpha = 108.721(5)°$, $\beta = 99.122(5)°$,

$\gamma = 98.695(6)^\circ$, $U = 922.50(18)$ Å^3, $T = 150(2)$ K, $P\bar{1}$, $Z = 2$, $\mu = 0.107\,\mathrm{mm}^{-1}$, $\lambda = 0.71073$ Å [Mo Kα], 19,211 reflections measured, 4408 unique ($R_{\mathrm{int}} = 0.0279$), observed 3488 ($I > 2\sigma(I)$). The final R_1 was 0.0448 (observed reflections 0.0588) and $wR(F^2)$ was 0.1114 (all data 0.1208) for 231 parameters. CCDC 795263 contains the supplementary crystallographic data for this paper. These data can be obtained free of charge from the Cambridge Crystallographic Data Centre via www.ccdc.cam.ac.uk/data_request/cif.

Acknowledgements

This work was supported by the EPSRC [EP/C007638/1].

References

(1) Ducharme, Y.; Wuest, J.D. *J. Org. Chem.* **1988**, *53*, 5787–5789.
(2) Etter, M.C. *Acc. Chem. Res.* **1990**, *23*, 120–126.
(3) Zimmerman, S.C.; Corbin, P.S. *Struct. Bond.* **2000**, *96*, 63–94.
(4) Prins, L.J.; Reinhoudt, D.N.; Timmerman, P. *Angew. Chem. Int. Ed.* **2001**, *40*, 2382–2426.
(5) Sijbesma, R.P.; Meijer, E.W. *Chem. Commun.* **2003**, 5–16.
(6) Sessler, J.L.; Jayawickramarajah, J. *Chem. Commun.* **2005**, 1939–1949.
(7) Sivakova, S.; Rowan, S.J. *Chem. Soc. Rev.* **2005**, *34*, 9–21.
(8) Wilson, A.J. *Soft Matter* **2007**, *3*, 409–425.
(9) de Greef, T.F.A.; Meijer, E.W. *Nature* **2008**, *453*, 171–173.
(10) Fox, J.D.; Rowan, S.J. *Macromolecules* **2009**, *42*, 6823–6835.
(11) van Esch, J.H.; Feringa, B.L. *Angew. Chem. Int. Ed.* **2000**, *39*, 2263–2266.
(12) Estroff, L.A.; Hamilton, A.D. *Chem. Rev.* **2004**, *104*, 1201–1218.
(13) Vishweshwar, P.; McMahon, J.A.; Bis, J.A.; Zaworotko, M.J. *J. Pharm. Sci.* **2006**, *95*, 499–516.
(14) MacGillivray, L.R.; Papaefstathiou, G.S.; Friši, T.; Hamilton, T.D.; Buar, D.-K.; Chu, Q.; Varshney, D.B.; Georgiev, I.G. *Acc. Chem. Res.* **2008**, *41*, 280–291.
(15) Gooch, A.; McGhee, A.M.; Renton, L.C.; Plante, J.P.; Lindsay, C.I.; Wilson, A.J. *Supramol. Chem.* **2009**, *21*, 12–17.
(16) McGhee, A.M.; Kilner, C.; Wilson, A.J. *Chem. Commun.* **2008**, 344–346.
(17) Legrand, Y.-M.; Michau, M.; van der Lee, A.; Barboiu, M. *Cryst. Eng. Commun.* **2008**, *10*, 490–492.